

# Towards Real-Time CFD Simulation of Indoor Environment

N. Morozova, R. Capdevila, F.X. Trias and A. Oliva  
Corresponding author: nina@cttc.upc.edu

Heat and Mass Transfer Technological Center (CTTC),  
Universitat Politècnica de Catalunya - BarcelonaTech (UPC)  
ESEIAAT, C/ Colom 11, 08222 Terrassa (Barcelona), Spain

**Abstract:** Growing computational power and improved numerical algorithms make Computational Fluid Dynamics (CFD) an attractive tool for simulations of indoor environment. In this study different turbulent models and discretization approaches are investigated on set of different mesh resolutions in order to choose the CFD technique that suits best for indoor environmental simulations. The investigated configuration is the tall differentially-heated cavity with height aspect ratio of 3.84, this configuration resembles a stratified indoor environment, such as a building atrium. The relative error of global airflow quantities is compared against computational time for different CFD approaches. LES simulations together with staggered discretization show the best overall performance in terms of computational speed and accuracy ratio. Furthermore the capability of CFD to perform real-time and even faster than real-time simulations is studied in paradigm of applying it for indoor environmental design and control systems.

*Keywords:* Indoor Environment Simulation, Large Eddy Simulation, Reynolds Averaged Navier-Stokes, Real-Time Simulation

## 1 Introduction

Heating, ventilation and air conditioning (HVAC) systems form a vital part of every modern building. These systems control main indoor air parameters (temperature, velocity, relative humidity, etc.) and create comfortable indoor environment. In all stages of HVAC project (from early conceptual design to detailed final plan), prediction of air distribution has key importance for the information concerning indoor air parameters. The fast computation of indoor airflow is of great interest in a vast number of applications in research and development, such as the design of efficient ventilation setups under the constraint of thermal comfort or the minimization of energy use, predictive control of building HVAC systems using real-time weather and occupants behaviour data.

Air distribution can be typically evaluated by analytical models, experimental measurements and computer simulations. The complexity of indoor airflow makes experimental or analytical investigation extremely difficult and expensive [1]. On the contrary, computer simulations are relatively cheap (depending on the chosen model type), easy to conduct and allow a high degree of flexibility addressing the problems. Multizone (airflow network) models, zonal models and Computational Fluid Dynamics (CFD) are the main tools for computer simulations of indoor environment. Multizone models have the lowest computational cost and the lowest accuracy, while CFD simulations provide detailed and accurate information about indoor air flow in cost of high computational effort.

Airflow network models represent the building as a network of well-mixed zones with uniform temperature, pressure and velocity. Zones are connected by the airflow paths with resistances. These models are based on Bernoulli equation, thus momentum effect is neglected. Due to the fact that each room is represented by a single node, thermal stratification and air velocity inside the rooms cannot be determined. Because of their

simplicity these models have severe limitations, which can produce significant errors in the results. Axley [2] provides a complete review of existing multizone models and their theoretical background.

Zonal models are considered the intermediate between airflow network and CFD. They divide a room into a limited number of cells and solve mass and energy balance equations in each cell. Zonal models either use momentum equation for the purpose of computational cost reduction. Hence, in case the flow momentum is strong, model accuracy could drop considerably. In order to improve simulation accuracy, regions with strong flow momentum are treated specially, which significantly increases the complexity of the method. High degree of case dependency prevents these models from gaining popularity. A review of existing zonal models can be found in [3].

In CFD simulations a system of partial differential equations is numerically solved for the conservation of mass, momentum and energy. Problem domain is divided into a mesh of control volumes and the equations are solved for each one of them. The solution provides a complete set of air parameters at every point of the domain. Effect of turbulence can be modelled using Direct Numerical Simulation (DNS), Large Eddy Simulation (LES) and Reynolds Average Navier-Stokes (RANS) approaches. DNS is the most accurate and the most computationally expensive method, because it directly resolves all the turbulent flow scales, which require very fine computational grids. LES models resolve only big scales of motion and model the small ones, while RANS numerically solve the mean flow and model its turbulent fluctuation. LES models are normally more computationally expensive than RANS, but both methods successfully reduce computational cost comparing to DNS. However, these CFD simulation models still have a huge data processing cost in comparison with multizone and zonal models.

Even though CFD is gaining popularity in the field of indoor environment simulations, the computing cost is still the main reason that prevents the usage of CFD for design and live control applications. However, nowadays there are three main CFD approaches, which have been used for addressing the problem of achieving correct detailed field of airflow parameters in real-time. Those are the lattice Boltzmann method (LBM), Fast Fluid Dynamics (FFD) and classical method based on finite-volume discretization together with turbulence modelling.

LBM has become increasingly popular [4, 5] over the last few years. Originating in the kinetic theory of gases it calculates the flow by means of the discretized Boltzmann equation. The fluid particles are forced to move on particular trajectories rather than moving in arbitrary directions. Macroscopic quantities such as pressure, temperature and velocity are obtained by particle distribution function. The numerical algorithm consists of two-steps: propagation and collision of fluid particles. It does not need iterations for the pressure calculation [6]. The method has parallel implementation on both central processing units (CPUs) and graphical processing units (GPUs) [7]. Despite efficient algorithms and parallelization, LBM is shown to be slower and less accurate than a coarse grid CFD simulation [4].

FFD was originally introduced by Stam [8] for computer games. Zuo & Chen [9] substantially improved the method by introducing turbulence modeling and applied the scheme to the airflow in buildings. The FFD method solves the advection term of Navier-Stokes equations with a first order semi-Lagrangian scheme, computes the diffusion term implicitly, and decouples pressure and velocity with a fractional step method [10]. The implicit scheme allows increased time step size, moreover computational speed is additionally increased by using low order discretization schemes. As a result FFD has a lower computing cost but also lower accuracy than the classic CFD does.

Capabilities of the CFD to simulate HVAC systems have been previously studied by Kempe & Hantsch [11]. They performed LES simulations of a model room with a heat source and concluded that real-time LES simulations can be carried out with high accuracy at moderate numerical effort. Nonetheless other turbulence models, like RANS, were not considered in their study. Wang & Zhai [12] examined the credibility of coarse-grid CFD simulations and optimized the space discretization in order to reduce the total truncation error. However, the detailed explanation of possible applications for building engineering was not highlighted in both research articles in details.

The capabilities of CFD to perform real-time simulations of indoor environment are investigated in this work. Different turbulence models and discretization techniques are tested, global flow quantities are evaluated in order to compare different simulations quality. The main objective of this study is to choose a reliable and robust model to perform CFD simulations of indoor environment with minimal computational cost and adequate accuracy. Moreover possibilities of using CFD simulation for design purposes and short-term thermal behaviour prediction in buildings HVAC control tools are discussed.

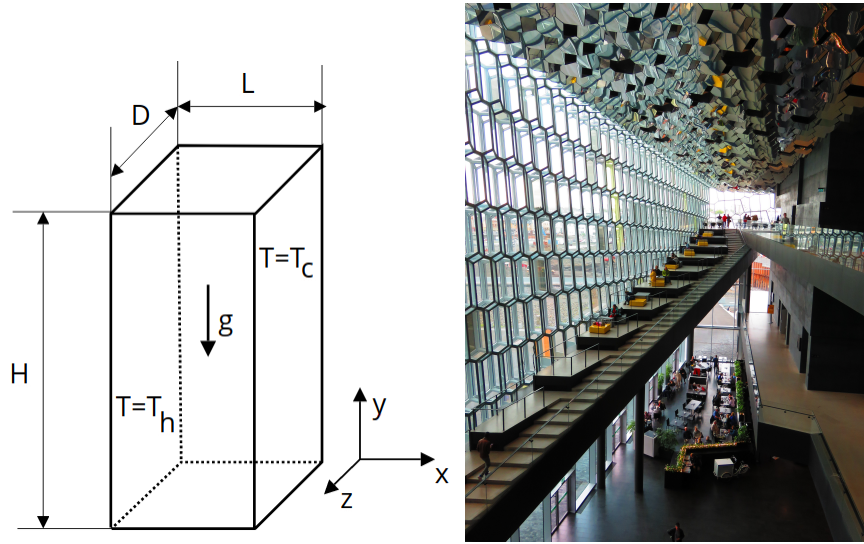


Figure 1: Left: Geometry definition of the simulated case. Right: Example of a building atrium [16].

The contents of this paper are organized as follows: Section 2 describes the details of the investigated physical problem and governing equations used. Section 3 shows numerical methods together with the software used for solving the physical problem. Section 4 shows the quality of numerical results obtained and describes the capabilities of CFD to perform real-time and faster than real-time simulations. Section 5 contains concluding remarks.

## 2 Physical problem and governing equations

A tall cavity, driven by the buoyancy forces is studied in this work. The objective of this flow configuration is to mimic a highly stratified turbulent indoor environment driven by natural convection. This type of flow pattern can be found in tall building atria, where one wall is exposed to solar radiation. Moreover this configuration could be used as a simplified model of a complete building. This flow configuration is very difficult to resolve correctly using multizone and zonal building modelling tools. At the same time erroneous predictions in the stratified indoor environment may lead to significant errors in the building HVAC design and later to low thermal comfort of inhabitants and high energy consumption.

The cavity has a height aspect ratio of  $A_h = H/L = 3.84$  and a depth aspect ratio of  $A_d = D/L = 0.86$  and is filled with air (Figure 1). The Prandtl number corresponds to air and is equal to  $Pr = 0.71$  and the Rayleigh number (based on the cavity height) is  $Ra = 1.2 \times 10^{11}$ . This configuration resembles the experimental set-up performed by Saury *et al.* [13].

Two opposite vertical walls of the cavity in the  $x$  direction are maintained at uniform but different temperatures  $T_h = 0.5$  at  $x = 0$  and  $T_c = -0.5$  at  $x = L$ . The temperature at the rest of the walls is given by the "Fully Realistic" boundary conditions (equations (1) and (2)) proposed in [14]. They are time independent analytical functions that fit the experimental data obtained by Salat *et al.* [15]:

$$\begin{cases} T(x^*, y^* = 0, z^*) = (0.5 - x^*) + 0.994 \frac{x^*(x^*-1)(x^*-0.681)}{x^*(x^*-1) - 0.0406(x^*+0.5)} \\ T(x^*, y^* = 1, z^*) = -T(1 - x^*, y^* = 0, z^*) \end{cases} \quad (1)$$

$$\begin{cases} T_1(x^*, y^*, z^* = 0/z^* = 1) = 0.5 - x^* + \frac{x^*(x^*-1)(-8.512+x^*(2.65-1.5y^*)+15.7y^*-7.539y^{*2})}{(x^*-1.01)(0.01+x^*)(0.85+0.5y^*)}, & \text{if } y^* \geq 0.9 \\ T_2(x^*, y^*, z^* = 0/z^* = 1) = 0.5 - x^* + \frac{0.7692x^*(x^*-1)(-0.8528+1.3x^*+0.4057y^*)}{(x^*-1.01)(0.01+x^*)}, & \text{if } 0.1 < y^* < 0.9 \\ T_3(x^*, y^*, z^* = 0/z^* = 1) = T_1(1 - x^*, 1 - y^*, z^* = 0/z^* = 1), & \text{if } y^* \leq 0.1, \end{cases} \quad (2)$$

Case	$N_x$	$N_y$	$N_z$	$N_{total}$	$(\Delta x)_{min}$
M0 (DNS)	450	900	256	$1.04 \times 10^8$	$4.28 \times 10^{-5}$
M1	8	30	4	$9.60 \times 10^2$	$7.97 \times 10^{-3}$
M2	10	40	6	$2.40 \times 10^3$	$5.67 \times 10^{-3}$
M3	12	50	8	$4.80 \times 10^3$	$4.46 \times 10^{-3}$
M4	14	60	10	$8.30 \times 10^3$	$3.65 \times 10^{-3}$
M5	18	80	12	$1.73 \times 10^4$	$2.70 \times 10^{-3}$
M6	24	100	16	$3.84 \times 10^4$	$1.89 \times 10^{-3}$
M7	30	120	20	$7.20 \times 10^4$	$1.49 \times 10^{-3}$
M8	40	150	24	$1.44 \times 10^5$	$1.08 \times 10^{-3}$
M9	50	180	30	$2.70 \times 10^5$	$8.10 \times 10^{-4}$
M10	70	240	40	$6.72 \times 10^5$	$5.40 \times 10^{-4}$
M11	100	320	40	$1.28 \times 10^6$	$4.05 \times 10^{-4}$

Table 1: Meshes used in the simulations.

where  $x^* = x/L, y^* = y/H, z^* = z/D$  are dimensionless spatial coordinates. Finally, no-slip boundary condition is imposed on the walls.

The incompressible Navier-Stokes equations for Newtonian flows with constant physical properties are considered. To account for the density variations, the Boussinesq approximation is adopted. Thermal radiation is neglected. Under these assumptions, the governing equations in dimensionless form are

$$\nabla \cdot \mathbf{u} = 0 \quad (3)$$

$$\frac{\partial \mathbf{u}}{\partial t} + (\mathbf{u} \cdot \nabla) \mathbf{u} = Pr Ra^{-1/2} \nabla^2 \mathbf{u} - \nabla p + \mathbf{f} \quad (4)$$

$$\frac{\partial T}{\partial t} + (\mathbf{u} \cdot \nabla) T = Ra^{-1/2} \nabla^2 T, \quad (5)$$

where  $\mathbf{u}$  is the velocity vector,  $t$  the time,  $p$  the pressure,  $T$  the temperature,  $\mathbf{f}$  is the body force vector, given by  $\mathbf{f} = (0, PrT, 0)$ ,  $Pr = \nu/\alpha$  is the dimensionless Prandtl number,  $\nu$  the kinematic viscosity,  $\alpha$  the thermal diffusivity,  $Ra = g\beta\Delta TH^3/(\nu\alpha)$  is the dimensionless Rayleigh number,  $g$  the gravitational acceleration,  $\beta$  the thermal expansion coefficient,  $H$  the reference length and  $\Delta T$  is the temperature difference,  $T_h - T_c$ . The reference time, velocity and temperature used for the dimensionless form are, respectively,  $Ra^{1/2}H^2\alpha^{-1}, Ra^{1/2}(\alpha/H), \Delta T$ . Hereafter, all the results are presented in dimensionless form.

Eleven different structured grids have been used in the numerical tests and are detailed in Table 1. All the grids are Cartesian, uniform in the vertical ( $y$ ) and normal ( $z$ ) directions and refined near the walls using a hyperbolic tangent function in the horizontal ( $x$ ) direction.

$$x = \frac{L}{2} \left( 1 + \frac{\tanh \gamma_x (2(i-1)/N_x - 1)}{\tanh \gamma_x} \right), \quad (6)$$

where the concentration factor is  $\gamma_x = 2$  for all meshes and  $N_x$  is the number of grid points in the horizontal direction.

LES simulations run for 1200 non-dimensional time units, which was found as the long enough time-integration period to reach statistically steady state behaviour. The physical time for RANS simulations is 250 non-dimensional time units, which is the approximate time for a fluid particle to complete a circle over the cavity.

### 3 Numerical methods

Three different software have been used to perform the simulations: OpenFOAM [17] for RANS approach using finite-volume discretization on collocated grid, TermoFluids software package [18] for LES turbulence models using finite-volume discretization on collocated grid and in-house software for LES/DNS simulations,

based on a symmetry-preserving finite volume discretization on structured staggered grids [19].

### 3.1 Reynolds-averaged Navier-Stokes approach

The RANS approach is based on time-averaged filtering of the governing equations (3) - (5). This approach calculates statistically-averaged (Reynolds-averaged) variables and simulates the turbulence fluctuation effect on mean airflow using different turbulence models. The time-averaged dimensionless governing equations (continuity, momentum and energy) of the fluid flow assuming fluid Newtonian behaviour and constant thermophysical properties are written as

$$\nabla \cdot \bar{\mathbf{u}} = 0 \quad (7)$$

$$\frac{\partial \bar{\mathbf{u}}}{\partial t} + (\bar{\mathbf{u}} \cdot \nabla) \bar{\mathbf{u}} = Pr Ra^{-1/2} \nabla^2 \cdot \bar{\mathbf{u}} - \nabla \bar{p} + \bar{\mathbf{f}} - \nabla \cdot \tau \quad (8)$$

$$\frac{\partial \bar{T}}{\partial t} + (\bar{\mathbf{u}} \cdot \nabla) \bar{T} = Ra^{-1/2} \nabla^2 \bar{T} - \nabla \cdot \mathbf{q} \quad (9)$$

$$\tau \approx -\nu_t (\nabla \bar{\mathbf{u}} + \nabla \bar{\mathbf{u}}^T) + \frac{2}{3} k I \quad \text{and} \quad \mathbf{q} \approx -\frac{\nu_t}{Pr_t} \nabla \bar{T}, \quad (10)$$

where overline  $\bar{\mathbf{u}}$ ,  $\bar{p}$  and  $\bar{T}$  are time average velocity, pressure and temperature respectively,  $\mathbf{f}$  is the body force vector, given by  $\mathbf{f} = (0, Pr\bar{T}, 0)$ . Modeled terms are the Reynolds stress tensor,  $\tau$ , and the turbulent heat flux,  $\mathbf{q}$ , where  $\nu_t$  is the turbulent viscosity,  $Pr_t$  is the turbulent Prandtl number,  $k$  the turbulent kinetic energy and  $I$  is the identity matrix.

RANS eddy-viscosity models are based on the resolution of turbulent viscosity by means of two different turbulent quantities: the turbulent kinetic energy ( $k$ ) and another turbulent quantity related to its dissipation. In case of  $k - \epsilon$  family of models it is dissipation rate of turbulent kinetic energy ( $\epsilon$ ), and for  $k - \omega$  models it is specific turbulent kinetic energy dissipation ( $\omega$ ).

The underlying assumption of the classic  $k - \epsilon$  model is that the turbulent viscosity is isotropic and the ratio between Reynolds stress and mean rate of deformations is the same in all directions. RNG  $k - \epsilon$  model results in a modified form of the classical model which attempts to account for the different scales of motion through changes to the production term. And SST  $k - \omega$  is the model, that combines the  $k - \omega$  and  $k - \epsilon$  turbulence model such that the  $k - \omega$  is used in the inner region of the boundary layer and switches to the  $k - \epsilon$  in the free shear flow.

In the present study three different RANS turbulence models have been tested, which were previously investigated by Zhai *et al.* [20, 21] for the HVAC applications. According to their recommendations, the family of two equations eddy-viscosity models has been chosen:  $k - \epsilon$  turbulence model [22], RNG  $k - \epsilon$  model [23] and SST  $k - \omega$  model [24].

RANS simulations are performed by the open source CFD code OpenFOAM [17] which is applied to collocated 3D meshes with finite-volume discretization. Transient "*buoyantBoussinesqPimpleFoam*" solver for buoyant, turbulent flow of incompressible fluids is chosen to solve pressure-velocity linkage in means of Boussinesq approximation and PIMPLE algorithm.

During the numerical experiments SST  $k - \omega$  model was systematically under-predicting overall heat transfer and showed highest computational cost among all three models. RNG  $k - \epsilon$  and  $k - \epsilon$  models showed similar performance in terms of accuracy, nonetheless  $k - \epsilon$  model had a lower computational cost. Thus  $k - \epsilon$  model is chosen for the further simulations and comparison with LES models.

### 3.2 Large Eddy Simulation approach

A different approach for turbulence modelling is the LES, where the large scale turbulent motions are resolved, whereas the effects of the smallest-scale motions are modelled by means of a subgrid-scale (SGS) model. In the present work four different SGS models have been tested: the wall-adapting local eddy-viscosity (WALE) SGS model [25], the variational multiscale method - WALE (VMS) SGS model [26], the QR model [27] and S3PQ model [28].

In WALE subgrid scale model the calculation of the eddy-viscosity,  $\nu_e$ , is based on the square of the velocity gradient tensor, which takes into account the shear stress tensor as well as the rotation tensor. In

WALE-VMS model three classes of scales are considered: large, small and unresolved scales. The first two classes are solved, whereas unresolved scales are modeled in restricted space of small scales using WALE approach. QR subgrid scale model is based on the invariants of the trace of square and cubic rate-of-stain tensor. S3PQ model uses a space of five invariants based on the symmetrical properties of gradient and divergence operators.

The spatial discretization in LES simulations is carried out using a symmetry preserving discretization on structured collocated [29] and staggered [30] Cartesian grids in order to test the stability of both methods in performing coarse grid simulations. Pressure and velocity coupling is solved using a fractional step method [10].

Adopting aforementioned approaches the dimensionless filtered Navier-Stokes equations are written as

$$\nabla \cdot \bar{\mathbf{u}} = 0 \quad (11)$$

$$\frac{\partial \bar{\mathbf{u}}}{\partial t} + (\bar{\mathbf{u}} \cdot \nabla) \bar{\mathbf{u}} = PrRa^{-1/2} \nabla^2 \bar{\mathbf{u}} - \nabla \bar{p} - \bar{\mathbf{f}} - \nabla \cdot \tau \quad (12)$$

$$\frac{\partial \bar{T}}{\partial t} + (\bar{\mathbf{u}} \cdot \nabla) \bar{T} = Ra^{-1/2} \nabla^2 \bar{T} - \nabla \cdot \mathbf{q} \quad (13)$$

$$\tau = \overline{\mathbf{u} \otimes \mathbf{u}} - \bar{\mathbf{u}} \otimes \bar{\mathbf{u}} \quad \text{and} \quad \mathbf{q} = \overline{\mathbf{u} T} - \bar{\mathbf{u}} \bar{T}, \quad (14)$$

where  $\bar{\mathbf{u}}$ ,  $\bar{T}$  and  $\bar{p}$  are respectively the filtered velocity, temperature and pressure and  $\mathbf{f} = (0, Pr\bar{T}, 0)$  is the body force vector. SGS tensor,  $\tau$ , and heat flux vector,  $\mathbf{q}$ , represent the effect of the unresolved scales and they need to be modeled in order to close the system. The most popular approach is the eddy-viscosity assumption:  $\tau \approx -\nu_e(\nabla \bar{\mathbf{u}} + \nabla \bar{\mathbf{u}}^T)$ ,  $\mathbf{q} \approx -\kappa_t \nabla \bar{T}$ , where  $\nu_e$  is the eddy-viscosity and  $\kappa_t$  is the eddy-diffusivity.

The aim of using two different discretization approaches is to test their effect on simulation results and speed. Discretization methods could have an important effect on the simulation stability and the results, especially for the coarser grids.

### 3.2.1 Large Eddy Simulation on a collocated structured grid

Large Eddy Simulations on a collocated structured grid using finite-volume approach [29] is carried out by the in-house CFD code Termofluids [18] which is a 3D parallel CFD object-oriented code applied to unstructured collocated meshes. One-parameter fully explicit second-order one-leg temporary discretization scheme [31] is used for time integration.

Two LES models have been tested on this code: WALE and WALE (VMS). Both models have given similar results, although the computational time for WALE model appeared to be shorter. A no model approach has also been tested. The absence of turbulence model brings instabilities for the coarse grids (M1-M5). LES-WALE model and no model are chosen for further tests.

### 3.2.2 Large Eddy Simulation on a staggered structured grid

A code based on a fourth-order symmetry-preserving finite volume discretization of the incompressible Navier-Stokes equations on structured staggered grids [30] is used to test WALE, QR and S3PQ turbulence models and no model approach. A second-order self-adapting explicit temporary discretization scheme [31] is used for the time integration. Details about the numerical algorithms and the verification [32] of this code are presented in Gorobets *et al.* [19].

All three LES models (WALE, QR and S3PQ) have shown similar results, but WALE model has had the highest computational cost and QR model has showed the least accurate results for the coarse meshes. S3PQ model is chosen for further simulations. The no model approach for the staggered grid has shown a similar to the S3PQ model performance.

## 4 Results

This section is dedicated to presentation of the simulation results, their convergence and the discussion on the possibility of real-time and faster than real-time CFD simulations. Results of CFD simulations with

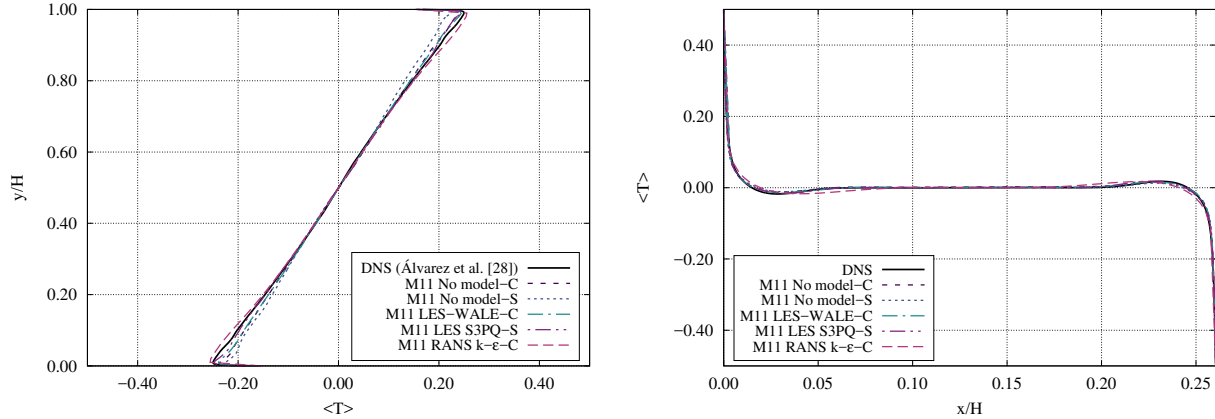


Figure 2: Averaged temperature profile at the cavity mid-depth ( $z/D = 0.5$ ). Left: at mid-width ( $x/L = 0.5$ ). Right: at mid-height ( $y/H = 0.5$ ).

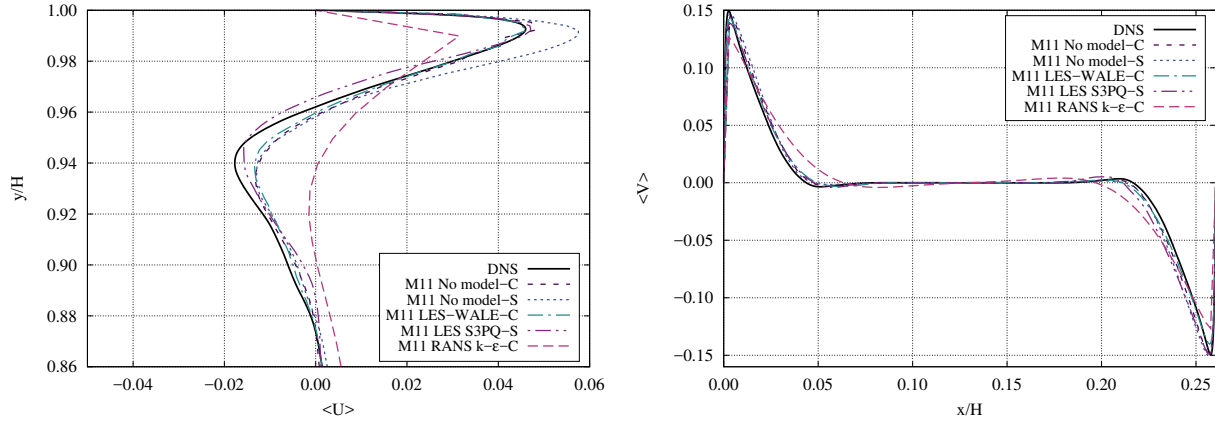


Figure 3: Left: averaged horizontal velocity profile at the cavity mid-depth ( $z/D = 0.5$ ) and mid-width ( $x/L = 0.5$ ). Right: vertical velocity profile at the cavity mid-depth ( $z/D = 0.5$ ) and mid-height ( $y/H = 0.5$ ).

different turbulence models and grids sizes are presented and discussed.

#### 4.1 Convergence study

Numerical results obtained with RANS, LES and no model approach for the finest grid M11 are compared against DNS data, obtained by the software described in the Section 3.2. [19]. DNS simulation results were partially published in [33]. The overall duration of DNS simulation is 600 non-dimensional time units. Grid resolution details are presented in Table 1.

Figures 2 - 3 display the time-averaged temperature field and velocity profiles at different cavity locations. All the values correspond to the time averaged flow, overlines "—" are omitted for the sake of clarity, brackets "<>" stand for the time averaged quantities. Obtained temperature and velocity profiles are in rather good agreement with the DNS simulation results.

The time averaged Nusselt number on the hot wall,  $Nu = \partial \langle T \rangle / \partial x$ , at the cavity mid-depth is displayed in Figure 4. LES and no models profiles are similar to the reference DNS result, but RANS simulation over-predicts the overall heat transfer. All simulations are able to predict the transition point and location of the peak value fairly well.

All LES and no model results are able to reproduce all flow features and show good convergence towards

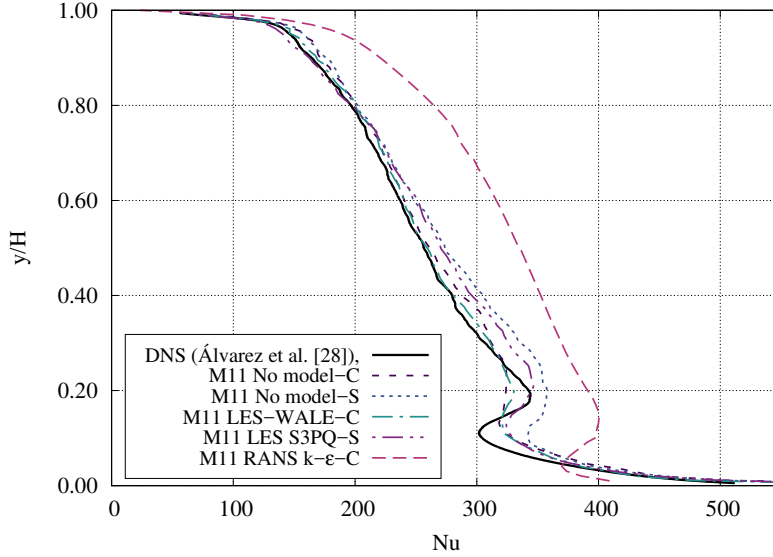


Figure 4: Averaged Nusselt number profile at the hot wall ( $x/L = 0.0$ ) at the cavity mid-depth ( $z/D = 0.5$ ).

DNS solution, however RANS results converge to a RANS solution of the flow.

## 4.2 Accessing real-time and faster than real-time simulations

The ability for real-time simulations is always a compromise between spatial and temporal resolution of the flow field, the available computing power, and the required accuracy. The focus of this paper is on the possibility of real-time CFD simulation on office workstation and not on high performance computers.

For the reason of speeding up the computation, all the simulations are preformed on the machine with AMD Opteron 2350 processor with  $24Gb/s$  memory bandwidth. The number of CPU cores, used for the parallel simulations is varied between 1 and 32. The computational time was then rescaled to the processor Intel Core i7-8700K with 6 CPU cores and  $41.6Gb/s$  memory bandwidth, which is a modern but affordable processor for an office workstation. The behaviour of the solvers has been assumed to be ideal, so simulations are re-scaled using linear dependencies of processors memory bandwidth, number of CPUs and number of nodes. Re-scaled target time,  $t_{tgt}$  is calculated as follows:

$$t_{tgt} = t_{ref} \frac{BW_{ref}}{BW_{tgt}} \frac{CPU_{ref}}{CPU_{tgt}} \frac{NODE_{ref}}{NODE_{tgt}}, \quad (15)$$

where  $t_{ref}, t_{tgt}$  are the reference and target computational time,  $BW_{ref}, BW_{tgt}$  the reference and target processor bandwidth,  $CPU_{ref}, CPU_{tgt}$  the reference and target number of CPUs and  $NODE_{ref}, NODE_{tgt}$  are the reference and target number of nodes respectively.

The indicator to evaluate the performance of the solvers is the time ratio  $R = t_{wc}/t_{phy}$  between the wall-clock time for the computation,  $t_{wc}$ , and physically simulated time,  $t_{phy}$ . A simulation is faster than real-time when  $R < 1$ .

The overall airflow pattern and global airflow quantities are more important for building simulations, than temperature and velocity profiles at specific locations. In order to evaluate the overall quality of the simulations, four global flow quantities are chosen for comparison: average Nusselt number, equation (16), average stratification (17), average kinetic energy (18), and average enstrophy (19). Average Nusselt number and stratification represent the thermal properties of the flow, average kinetic energy is used to quantify the overall level of motion and average enstrophy corresponds to dissipation effects in the fluid.

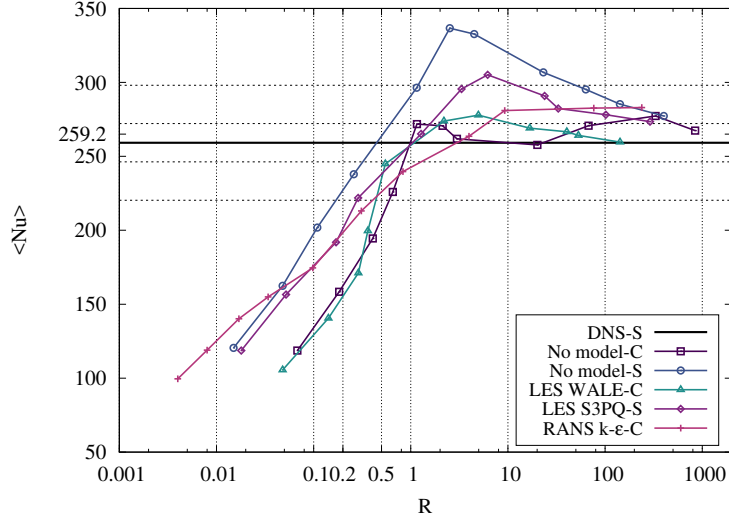


Figure 5: Average Nusselt number,  $\langle Nu \rangle$ , for different grid resolutions (Table 1) and turbulence models against the time ratio  $R$ .

$$\langle Nu \rangle = \int_0^1 \frac{\partial \langle T \rangle}{\partial x} dy \Big|_{x=0} \quad (16)$$

$$\langle S \rangle = \frac{\partial \langle T \rangle}{\partial y} dx \Big|_{y=0.5} \quad (17)$$

$$\langle E \rangle = \int_V \frac{\langle \mathbf{u}^2 \rangle}{2} dV \quad (18)$$

$$\langle \Omega \rangle = \int_V \langle \boldsymbol{\omega}^2 \rangle dV, \quad (19)$$

where  $V$  is the volume of the cavity and  $\boldsymbol{\omega}$  is the vorticity.

In Figures 5 - 8 these quantities are plotted against the computational time ratio  $R$  in logarithmic scale. Each point of the graph represents a mesh from Table 1. The horizontal dash lines separate the area within 5% and 15% error from reference value, obtained by DNS simulations (thick black line).

In general all the turbulence models have predicted average Nusselt number rather well (Figure 5). All approaches show very low values of  $\langle Nu \rangle$  on the coarse grids, but from mesh M5 onward results already fall in the 15% error range. But no model approach on staggered grid overpredicts  $\langle Nu \rangle$  for meshes M5-M8, but for finer meshes its values get closer to the reference. Despite the lowest computational cost, RANS simulation shows the slowest convergence. In overall LES models for both collocated and staggered approach, and no model approach on collocated grid, show the best results and perform faster than real-time simulations with less than 15% relative error.

Average stratification (Figure 6) is converging to the reference value in an oscillating way for most approaches, though RANS  $k - \epsilon$  model demonstrates smoother behaviour. The oscillating behavior of stratification is originating in fact that this is not strictly a global quantity, because it is evaluated only in the cavity mid height ( $y/H = 0.5$ ) and mid width ( $x/L = 0.5$ ). Therefore, all the approaches, except the no model on staggered grid, performed faster than real-time simulations with about 15% relative error.

Average kinetic energy (Figure 7) is well predicted by the RANS  $k - \epsilon$  model and LES-S3PQ model on staggered grid. Both models are able to perform faster than real-time simulations with reasonable relative error. LES-WALE model has not shown a good convergence, and both no model approaches failed to predict average kinetic energy  $\langle E \rangle$  correctly.

Average enstrophy (Figure 8) is the global quantity, which appeared to be the most difficult to be

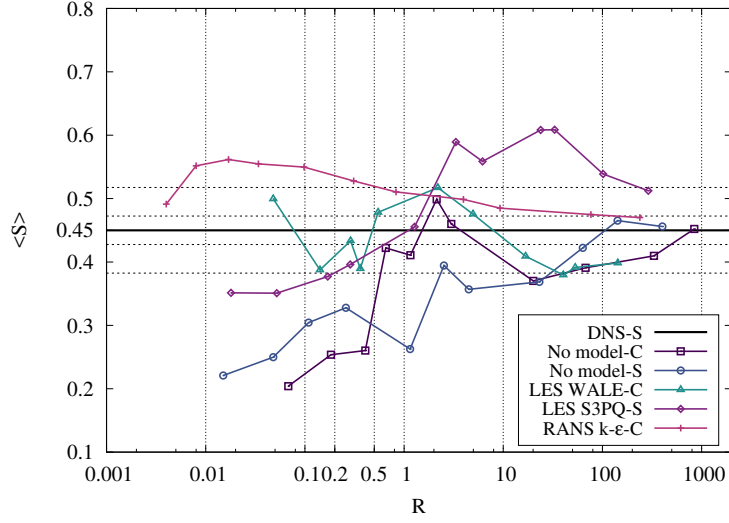


Figure 6: Average stratification,  $\langle S \rangle$ , for different grid resolutions (Table 1) and turbulence models against the time ratio  $R$ .

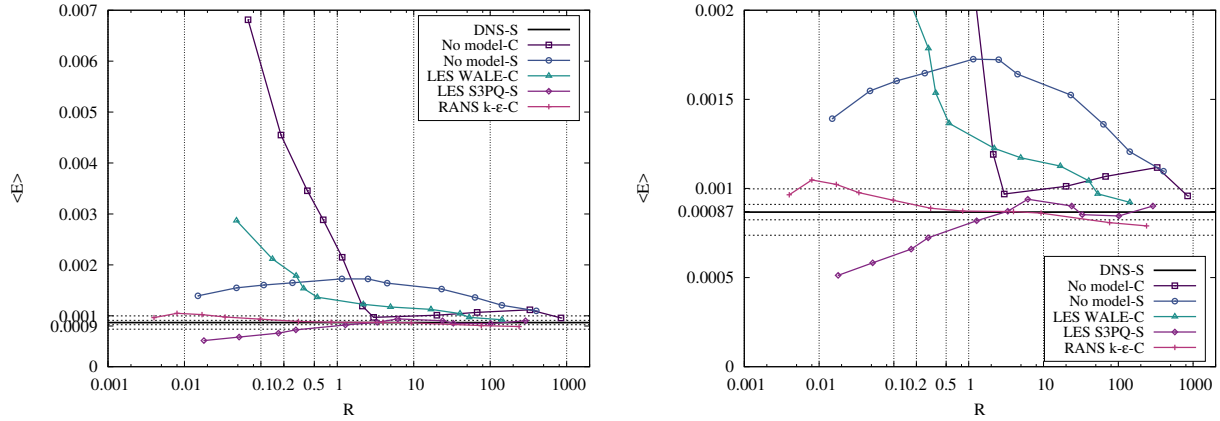


Figure 7: Left: Average kinetic energy,  $\langle E \rangle$ , for different grid resolutions (Table 1) and turbulence models against the time ratio  $R$ . Right: Zoomed image of the graph on the left

predicted correctly. However both LES-S3PQ and no model on staggered grid have given good results, while a collocated grid approach has not shown a stable convergence behavior. RANS  $k - \epsilon$  model has failed to give correct values of the enstrophy.

From the simulation results could be concluded, that RANS  $k - \epsilon$  model has the lowest computational cost on the coarse grids, but the cost increases significantly with the mesh resolution. In spite of a relatively low computational cost, the accuracy of the RANS simulations remains limited. Simulation without turbulence model on collocated grid has a good computational cost and accuracy ratio, but shows an unstable behaviour on the coarse grids. But the same approach on staggered grid has more stable behaviour. Both LES models show similar level of accuracy, nonetheless, the staggered discretization approach is more accurate and faster on coarse grids. LES simulation with S3PQ turbulent model shows the best overall performance in terms of computational cost and accuracy.

The experiment performed by Saury *et al.* [13] had a temperature difference between hot and cold walls of  $\Delta T = 20^\circ C$ . This temperature difference corresponds to the air-filled cavity of the size  $L \times H \times D = 1.00 \times 3.84 \times 0.86$  meters. A temperature difference of  $20^\circ C$  is relatively high for indoor environments. As an example of real indoor environment, a building atrium exposed to the hot summer temperature of

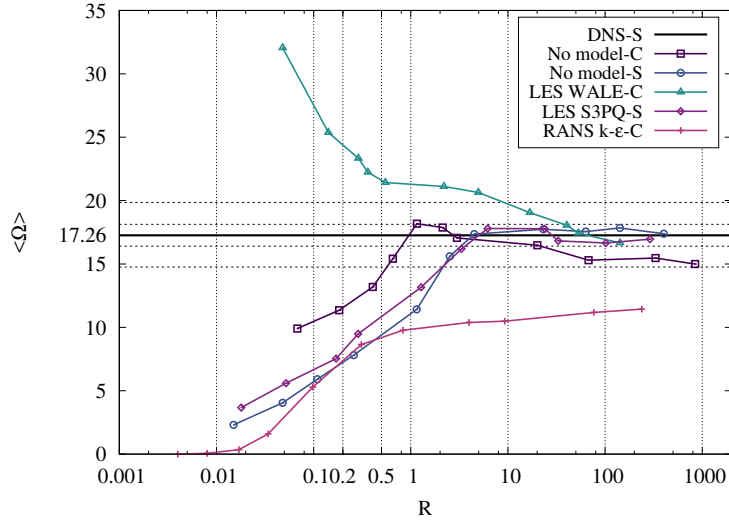


Figure 8: Average enstrophy,  $\langle \Omega \rangle$ , for different grid resolutions (Table 1) and turbulence models against the time ratio  $R$ .

$T_{hot} = 28^{\circ}C$  on one side and maintained at the constant temperature of an air conditioned building of  $T_{cold} = 23^{\circ}C$  could be taken. The simulated domain size would become equal to  $1.59 \times 6.10 \times 1.37$  meters, which could correspond to a two floor high atrium or a staircase. The simulated case is challenging because of high level of stratification and high aspect ratio, but in many real indoor environments aspect ratio and stratification are lower, which would reduce the computational cost and difficulty of prediction.

Assuming that the computational cost scales linearly with the volume, simulations could be extrapolated to the scale of a complete building. A typical four floors residential building would have a size of approximately  $L \times H \times D \approx 10 \times 10 \times 10$  meters and a volume of  $1000m^3$ , which is approximately 75 times bigger than simulated cavity.

#### 4.2.1 Potential of real-time simulations for design purposes

CFD simulations are not yet widespread in the building application area. Detailed building project in many cases requires an annual indoor environment simulations [34], which is too computationally expensive. The annual simulation could be replaced by several representative daily simulations [35] (a typical summer day, a typical winter day, etc.). A 24 hours simulation with adequate computational time and accuracy is not an impossible task for the CFD, for this reason this paper is focused on the design applications for representative daily simulations.

Design of HVAC systems is normally divided into two stages: early conceptual design and final detailed design. Early stage conceptual design does not require high accuracy. At this stage of a project only conceptual engineering decisions are made. Much more important for conceptual design is the ability to predict overall airflow patterns and global flow quantities with reasonable time of calculation. An assumption of 15% acceptable relative error is adopted for this design stage. Unlike early stage conceptual design applications, the final stage design applications require accurate and detailed simulation results, as a result global quantities relative error is assumed to remain below 5% [34].

The assumed reasonable computational speed for design application is two times faster than a real-time ( $R \leq 0.5$ ). The idea behind the design time ratio of ( $R \leq 0.5$ ) is the possibility for an engineer to start a 24 hours physical period of time,  $t_{phy}$ , simulation at the end of the working day and receive results the next morning (in 12 hours approximately).

According to the results presented in Figures 5 - 8, grid M5 (Table 1) with 17280 control volumes would be fine enough for the early design stage simulations. Typically big computational resources are not available for early design stage, so above mentioned office workstation with 6 cores is able to perform a CFD simulation with LES-S3PQ turbulence model on staggered grid with the time ratio of  $R \approx 1.3$ . The the wall-clock time,

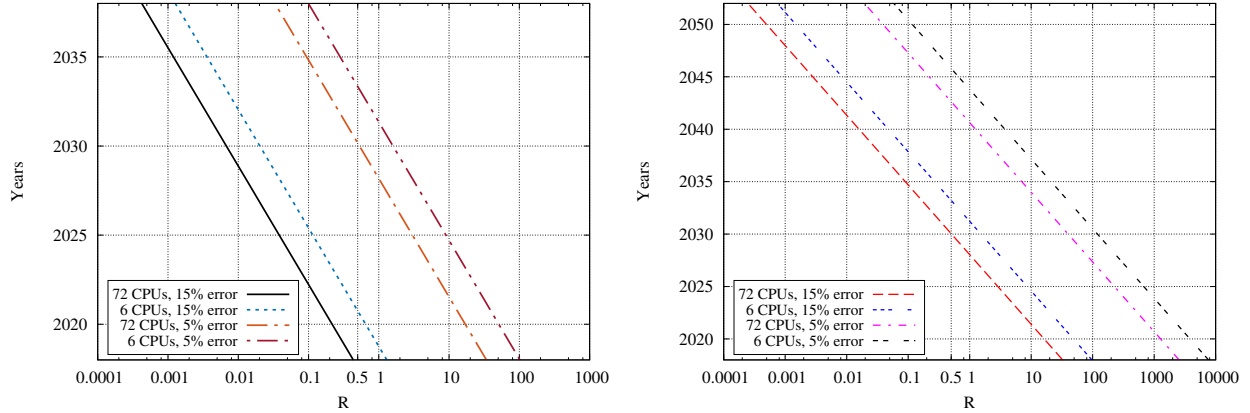


Figure 9: Potential of accessing real-time and faster than a real-time CFD simulations over the next years. Left: Simulated problem. Right: An estimation for a residential building.

$t_{wc} = 1533$  seconds, is approximated using equation (15) and the physical time is equal to  $t_{phy} = 1200$  time units.

However a final detailed design stage needs a finer grid resolution, computational grid M10 (Table 1) with 672000 control volumes, which produce less than 5% relative error, would be suitable for this purpose. Its computational time ratio for the 6 cores office workstation would and LES-S3PQ model on staggered grid be  $R \approx 100$  (Figures 5 - 8). The the wall-clock time for this simulation is 122057 seconds, and the physical time is equal to  $t_{phy} = 1200$  time units. Taking into account the availability of bigger computational resources for the final detailed simulations, the time ratio could be decreased using four Intel Core i9-7980XE Extreme Edition Processors with 18 CPUs each and 41.6Gb/s memory bandwidth. Applying the equation (15) the wall-clock time becomes  $t_{wc} = 40690$  seconds, so the time ratio decreases to  $R \approx 34$  respectively.

At this moment CFD simulations for design purposes are not possible neither for final detailed design nor for early conceptual design. Taking into account the Moore's law [36], which stands that the number of transistors in a dense integrated circuit doubles about every two years, time in which CFD applications for design purposes would be available could be estimated.

Figure 9 shows the decreasing simulation time ratio (due to the growing computational power) over the years for different relative errors and different number of CPUs. Values for the year 2018 are obtained during the simulations and can be viewed on the Figures 5 - 8, values for the future years are extrapolated using the Moore's law.

CFD simulations for early design stage applications on the office workstation would be possible in less than 5 years (Figure 9). Yet simulations for detailed indoor environment design on the office workstation would be possible in two decades, but using four 18 cores processors, CFD would be available for detailed design simulations in approximately 15 years (Figure 9).

Taking into account the aforementioned assumption of a real building with a volume of  $100m^3$  (75 times bigger than simulated cavity), the simulation time ratio would grow linearly and reach  $R \approx 100$  for early design stage simulations,  $R \approx 7650$  for detailed design on the office workstation and  $R \approx 2550$  for detailed design using 72 CPU cores. So CFD simulations for a complete building would be available in less than 10 years for early design stage and in approximately 15 years for detailed design (Figure 9).

#### 4.2.2 Model predictive control applications

In order to incorporate CFD simulations into building energy control systems, they should be even faster than design applications. Model predictive control (MPC) systems for buildings require a resolved airflow at least 15 minutes before the signal would be sent to the building HVAC system [34]. For the proper control of the building energy demand is assumed that CFD simulation could be ten times faster than the real-time ( $R \leq 0.1$ ), in order to receive resolved airflow in 1.5 minutes and send a signal into the system 15 minutes before the change in the boundary conditions.

At the same time all simulations should be performed using office workstation computers. Required simulation accuracy highly depends on the controlled building function: Civil buildings like offices or residential buildings have a bigger range of acceptable air parameters, than, for example, hospitals or server rooms do.

With the current computational power it is not possible to incorporate CFD simulations into MPC system of a building, but with growing processors capacity it would be possible to predict and control air parameters for civil buildings with LES-S3PQ model on staggered grid and with 5% relative error [34] within two decades (Figure 9). For the real building size the MPC system application would become available within three decades (Figure 9).

## 5 Conclusions

CFD simulations are the promising tool for air distribution prediction in indoor environment. They provide users with a complete set of air parameters, which could be used for design and control purposes. Unlike other building simulation models, CFD is able to resolve highly stratified indoor environments and other complex flow configurations.

Turbulence modelling in CFD simulations is important for their quality, simulations without turbulence model do not predict airflow distribution correctly on coarse grids and require very small time step in order to produce acceptable results. LES turbulence models in overall show better performance than RANS: although RANS models have lower computational cost on coarser grids, their capacity to predict airflows correctly is limited. All LES models provided similar results, but important point in reducing the computational cost and maintaining the simulations stability is using a staggered symmetry-preserving discretization approach on coarser grids together with turbulence modelling.

At this moment CFD simulations are not affordable neither for design nor for control of indoor environment. But with growing computer capacity CFD would be feasible for design purposes on office workstations within the next decade for the investigated cavity and within two decades for an arbitrary residential building. While HVAC predicting control systems equipped with CFD simulation tools will get affordable in approximately two-three decades.

It is important to mention that the effect of solar radiation, occupants behaviour, equipment heat emissions, etc. was not considered in the present work. All these factors would complicate CFD simulations of indoor environment. However the computational time ratio could be decreased by using modern processors with more cores and by improving numerical algorithms and discretization techniques.

In the future work the problems analyzed would be extended to ventilated cavities with heat sources (mimicking occupants behavior, solar radiation and heat emissions from the equipment) and domains with complicated geometry. Other interesting way for future work would be the analysis of the simulations financial costs in terms of electrical power spent per CPU hour. The third and the most important direction for the future work is the optimization of existing numerical algorithms and their GPU acceleration using a fully-portable, algebra-based framework for heterogeneous computing developed by Álvarez *et. al* [33].

## 6 Acknowledgments

This work has been financially supported by the Ministerio de Economía y Competitividad, Spain (No.ENE2017-88697-R). N.M. is supported by a FPU 2016 predoctoral contract (NoFPU16/06333) financed by Ministerio de Economía y Competitividad, Spain. F.X.T. is supported by a Ramón y Cajal postdoctoral Contract (No. RYC-2012-11996) financed by the Ministerio de Economía y Competitividad, Spain.

## References

- [1] Q. Chen. Ventilation performance prediction for buildings: A method overview and recent applications. *Building and Environment*, 44(4):848–858, 2009.
- [2] J. Axley. Multizone Airflow Modeling in Buildings: History and Theory. *HVAC&R Research*, 13(6):907–928, 2007.

- [3] A.C. Megri and H. Fariborz. Zonal Modeling for Simulating Indoor Environment of Buildings: Review, Recent Developments, and Applications. *HVAC&R Research*, 13(6):887–905, 2007.
- [4] B. Elhadidi and H.E. Khalifa. Comparison of coarse grid lattice Boltzmann and Navier Stokes for real time flow simulations in rooms. *Building Simulation*, 6(2):183–194, 2013.
- [5] M.A.I. Khan, N. Delbosc, C.J. Noakes, and J. Summers. Real-time flow simulation of indoor environments using lattice Boltzmann method. *Building Simulation*, 8(4):405–414, 2015.
- [6] S. Chen and G.D. Doolen. Lattice Boltzmann Method for fluid flows. *Annual Review of Fluid Mechanics*, 30:329–364, 1998.
- [7] F. Kuznik, C. Obrecht, G. Rusaouen, and J.-J. Roux. LBM based flow simulation using GPU computing processor. *Computers and Mathematics with Applications*, 59:2380–2392, 2010.
- [8] J. Stam. Stable fluids. In *Proceedings of the 26th Annual Conference on Computer Graphics and Interactive Techniques*, pages 121–128, 1999.
- [9] W. Zuo and Q. Chen. Real-time or faster-than-real-time simulation of airflow in buildings. *Indoor Air*, 19(1):33–44, 2009.
- [10] A. Chorin. A Numerical Method for Solving Incompressible Viscous Flow Problems. *Journal of Computational Physics*, 135:118–125, 1967.
- [11] T. Kempe and A. Hantsch. Large-eddy simulation of indoor air flow using an efficient finite-volume method. *Building and Environment*, 115:291–305, 2017.
- [12] H. Wang and Z. Zhai. Application of coarse-grid computational fluid dynamics on indoor environment modeling: Optimizing the trade-off between grid resolution and simulation accuracy. *HVAC&R Research*, 18(5):915–933, 2012.
- [13] D. Saury, N. Rouger, F. Djanna, and F. Penot. Natural convection in an air-filled cavity: Experimental results at large Rayleigh numbers. *International Communications in Heat and Mass Transfer*, 38(6):679–687, 2011.
- [14] A. Sergent, P. Joubert, S. Xin, and P. Le Quéré. Resolving the stratification discrepancy of turbulent natural convection in differentially heated air-filled cavities Part II: End walls effects using large eddy simulation. *International Journal of Heat and Fluid Flow*, 39:15–27, 2013.
- [15] J. Salat, S. Xin, P. Joubert, A. Sergent, F. Penot, and P. Le Quéré. Experimental and numerical investigation of turbulent natural convection in a large air-filled cavity. *International Communications in Heat and Mass Transfer*, 25:824–832, 2004.
- [16] PEXELS. Copyright free images database. [<https://www.pexels.com/photo/interior-of-railroad-station-258626/>].
- [17] OpenFOAM. The OpenFOAM Foundation. [<https://openfoam.org/>].
- [18] Termo Fluids S.L. Termofluids. [<http://www.termofluids.com/>].
- [19] A. Gorobets, F.X. Trias, M. Soria, and A. Oliva. A scalable parallel Poisson solver for three-dimensional problems with one periodic direction. *Computers & Fluids*, 39:525–538, 2010.
- [20] Z.J. Zhai, Z. Zhang, W. Zhang, and Q.Y. Chen. Evaluation of Various Turbulence Models in Predicting Airflow and Turbulence in Enclosed Environments by CFD: Part 1 - Summary of Prevalent Turbulence Models. *HVAC&R Research*, 13(6):853–870, 2007.
- [21] Z.J. Zhai, Z. Zhang, W. Zhang, and Q.Y. Chen. Evaluation of Various Turbulence Models in Predicting Airflow and Turbulence in Enclosed Environments by CFD: Part 2 - Comparison with Experimental Data from Literature. *HVAC&R Research*, 13(6):871–886, 2007.
- [22] B.E. Launder and B.I. Spalding. The numerical computation of turbulent flows. *Computer methods in Applied Mechanics and Energy*, 3:269–289, 1974.
- [23] V. Yakhot and S.A. Orszag. Renormalization group analysis of turbulence. *Journal of Scientific Computing*, 1:3–51, 1986.
- [24] F.R. Menter. Two-equation eddy-viscosity turbulence model for engineering applications. *AIAA Journal*, 32:1598–1605, 1994.
- [25] L. Bricteuxa, M. Duponcheel, and G. Winckelmans. A multiscale subgrid model for both free vortex flows and wall-bounded flows. *Physics of Fluids*, 21:105102, 2009.
- [26] T.J.R. Hughes, L. Mazzei, and K.E. Hanzen. Large Eddy Simulation and the variational multiscale method. *Computing and Visualization in Science*, 3(1):47–59, 2000.
- [27] R. Verstappen. When Does Eddy Viscosity Damp Subfilter Scales Sufficiently? *Journal of Scientific Computing*, 49:94–110, 2011.

- [28] F.X. Trias, D. Folch, A. Gorobets, and A. Oliva. Building proper invariants for eddy-viscosity subgrid-scale models. *Physics of Fluids*, 27:065103, 2015.
- [29] F.X. Trias, O. Lehmkuhl, A. Oliva, C.D. Pérez-Segarra, and R.W.C.P. Verstappen. Symmetry-preserving discretization of Navier-Stokes equations on collocated unstructured grids. *Journal of Computational Physics*, 258(1):246–267, 2014.
- [30] R.W.C.P. Verstappen and A.E.P. Veldman. Symmetry-preserving discretization of turbulent flow. *Journal of Computational Physics*, 187:343–368, 2003.
- [31] F.X. Trias and O. Lehmkuhl. A self-adaptive strategy for the time-integration of Navier-Stokes equations. *Numerical Heat Transfer, part B*, 60(6):116–134, 2011.
- [32] F.X. Trias, M.Soria, A. Oliva, and C.D. Pérez-Segarra. Direct numerical simulations of two- and three-dimensional turbulent natural convection flows in a differentially heated cavity of aspect ratio 4. *Journal of Fluid Mechanics*, 586:259–293, 2007.
- [33] X. Álvarez, A. Gorobets, F. X. Trias, R. Borrell, and G. Oyarzun. HPC2 - a fully portable algebra-dominant framework for heterogeneous computing. Application to CFD. *Computers & Fluids*, 000:1–8, 2018.
- [34] F. Ferracuti, A. Fonti, L. Ciabattini, S. Pizzuti, A. Arteconi, L. Helsen, and G. Comodi. Data-driven models for short-term thermal behaviour prediction in real buildings. *Appl. Energy*, 204:1375–1387, 2017.
- [35] O. Neu, S. Oxizidis, D. Flynn, F. Pallonetto, and D. Finn. High resolution space - time data: Methodology for residential building simulation modelling. In *Proceedings of 13th Conference of International Building Performance Simulation Association*, August 26-28 2013.
- [36] G. E. Moore. The future of integrated electronics. Technical report, Palo Alto, CA, USA, 1965.